Supporting Information

Gate-Induced Metal-Insulator Transition in 2D Van der Waals Layers of Copper Indium Selenide ($CuIn_7Se_{11}$) Based Field-Effect Transistors (FETs)

Prasanna D. Patil[1], Sujoy Ghosh[1]*, Milinda Wasala[1]*, Sidong Lei[2,3], Robert Vajtai[2], Pulickel M. Ajayan[2], Arindam Ghosh,[4,5] Saikat Talapatra[1#]

[1]Department of Physics, Southern Illinois University Carbondale, Carbondale, IL-62901, USA.
[2]Department of Materials Science and Nanoengineering, Rice University, Houston, TX-77005, USA.
[3]Department of Physics and Astronomy, Georgia State University, Atlanta, GA-30303, USA
[4]Department of Physics, Indian Institute of Science, Bangalore 560012, India.
[5]Centre for Nano Science and Engineering, Indian Institute of Science, Bangalore 560012, India.

* Equally Contributing Authors

Corresponding Author. Email: saikat@siu.edu

I. Y-function Method for estimating contact resistance.

Y-function method, as first demonstrated by Ghibaudo[1] and modified by Chang *et.al*,[2] to include gate dependent Schottky barrier, was used to evaluate low-field mobility (μ_0) and estimate effective contact resistance (R_C) in strong inversion region ($V_g >> V_d$). Detailed derivation of Y-function method can be found in ref 2. For low-field bias condition ($V_g >> 0.5V_d$), drain current can be writes as Equation S.I.1,

$$I_d = \left(\frac{\mu_0}{1+\theta\left(V_g - V_{th}\right)}\right) C_{ox}\, V_d\, \frac{W}{L}\left(V_g - V_{th}\right) \tag{S.I.1}$$

where all symbols carry their usual meaning and θ is effective attenuation factor, express as $\theta = \theta_0 + \mu_0.R_C.C_{ox}.W/L$ and θ_0 is first-order mobility attenuation coefficient. In general case, Y-function, which is defined as $I_d/\sqrt{g_m}$ (g_m is transconductance, $\partial I_d/\partial V_g$) is given by Equation S.I.2,

$$Y = \frac{I_d}{\sqrt{g_m}} = \frac{\sqrt{\mu_0\, C_{ox}\, V_d\, \frac{W}{L}}}{\sqrt{1 - \mu_0\, C_{ox}\, R'_C\, \frac{W}{L}\, (V_g - V_{th})^2}} (V_g - V_{th}) \tag{S.I.2}$$

where R'_C is $\partial R_C/\partial V_g$. For our device, we found that effective Schottky barrier is almost constant for $V_g > 15$ V thus contact resistance (R_C) will be independent of applied gate voltage (V_g) in strong inversion region ($V_g >> V_d$). Thus Equation S.I.2 can be written as Equation S.I.3,

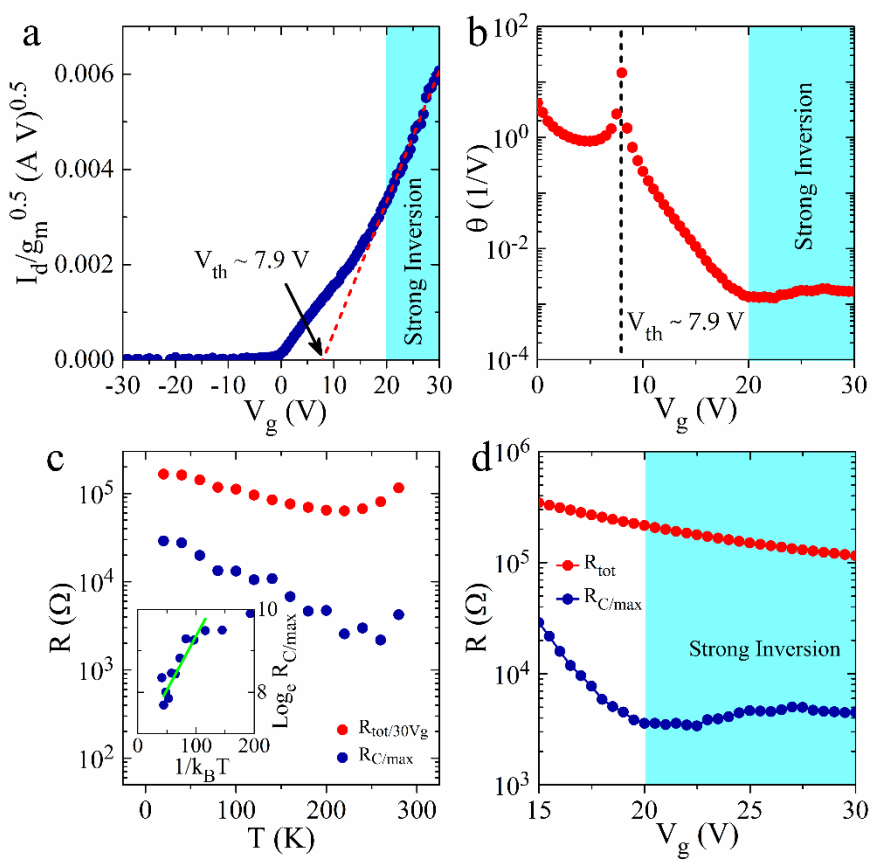

Figure S1: Y-function analysis of $CuIn_7Se_{11}$ FET a) Y-function as a function of gate voltage. b) effective attenuation factor as function of gate voltage. c) & d) Comparison of upper limit of contact resistance and total resistance of device (channel plus contact) as a function of gate voltage (c) and as a function of temperature (d). Inset of d) contact resistance in log scale as a function of $1/k_BT$, slope of fit (green line) estimates Schottky barrier height (Φ_{SB}).

$$Y = \frac{I_d}{\sqrt{g_m}} = \sqrt{\mu_0 \, C_{ox} \, V_d \, \frac{W}{L}} \left(V_g - V_{th}\right) \tag{S.III.3}$$

Figure S1 shows Y-function analysis of device presented in main manuscript. Plot of Y-function as a function of applied gate voltage (V_g) at 280 K is shown in Figure S1a. In the strong inversion region (represented by cyan background), data is fitted to linear fit according to Equation S.I.3 and threshold voltage, V_{th} ~ 7.9 V and low-field mobility, μ_0 ~ 24.13 cm^2 V^{-1} s^{-1} were estimated from slope and intercept of linear fit, respectively. Values of threshold voltage estimated from transfer curve (V_{th} ~ 8 V) and Y-function (V_{th} ~ 7.9 V) are matching. Also, field-effect mobility (μ_{FE} ~ 25.9 cm^2 V^{-1} s^{-1}) and low-field mobility (μ_0 ~ 24.13 cm^2 V^{-1} s^{-1}), indicating that contact resistance is negligible for our device.[2]

Further, we estimated effective attenuation factor (θ) as a function of voltage, as shown in Figure S1a. In the limit of negligible θ_0, maximum contact resistance ($R_{C/max}$) can be estimated from $\theta \approx \mu_0.R_{C/max}.C_{ox}.W/L$. Maximum contact resistance ($R_{C/max}$) as well as total resistance of FET, $R_{tot} = V_d/I_d$, is shown in Figure S1c. We found that, at 280 K, $R_{C/max}$ ~ 4.3 kΩ is more than an order of magnitude lower than R_{tot} ~ 115 kΩ at V_g = 30 V. Thus we can conclude that electronic properties of our $CuIn_7Se_{11}$ FET is not governed by contact. Dependence of $R_{C/max}$ on temperature is shown in Figure S1d. We found that contact resistance was at least order of magnitude lower than R_{tot} at V_g = 30 V for all temperatures. Increase in contact resistance with decrease in temperature is a common signature of thermionic emission at metal-semiconductor junction [3], thus we have used thermionic emission and 2D Richardson equation to determine Schottky barrier height (details in later). According to thermionic emission,[3]

$$R_C = R_0 \, e^{\Phi_{SB}/k_B T} \tag{S.III.4}$$

Upon fitting $R_{C/max}$ with $1/k_BT$ (inset of Figure S1d), Schottky barrier height (Φ_{SB}) was estimated to be 26 meV which is comparable with Φ_{SB} ~ 25 meV estimated from 2D Richardson equation.

II. Thermionic emission and Schottky barrier

Metal-semiconductor junction plays a key role in determining electron transport in devices.[4] Schottky barrier at metal-semiconductor junction can affect electron injection in semiconducting channel from metal contacts. Schottky barrier height will depending Fermi energy of semiconductor and work function of metal. Higher mismatch will result in higher barrier height (Φ_{SB}). Presence of Schottky barrier will reflect electron back into contact, though usually thermal energy is sufficient enough to promote carrier to cross barrier by thermionic emission process. With application of gate voltage, Fermi energy can be modulated resulting in change in 'apparent' barrier height (Φ_B). At higher gate voltages, tunneling across barrier takes over thermionic emission. Thus, at intermediate gate voltages, flat band condition is reached, and barrier height extracted from thermionic emission is actual Schottky barrier height (Φ_{SB}).[4] Thus, it is utmost important to understand charge transport at channel-contact junction.

In case of 2D materials, thermionic process follows 2D Richardson equation[5, 6], given by Equation S.II.1,

$$I_d = A\,A^*\,T^{3/2}\,exp\left[-\frac{e}{k_BT}\left(\Phi_B - \frac{V_d}{n}\right)\right] \tag{S.II.1}$$

Where, A is the contact area, A^* is the Richardson constant, e is electron charge and n is the ideality factor. Ideality factor for our $CuIn_7Se_{11}$ FET was estimated to be n ~ 8.6 by using Cheung's function,[7, 8] as shown in Equation S.II.2,

$$\frac{\partial V_d}{\partial \ln(I_d)} = n\frac{k_B T}{e} + I_d\, R_s \tag{S.II.2}$$

Where R_s is series resistance. Figure S2a shows a plot of $I_dT^{-1.5}$ in logarithmic scale as a function of $1/k_BT$ for various applied gate voltages ranging from 0 V to 30 V.

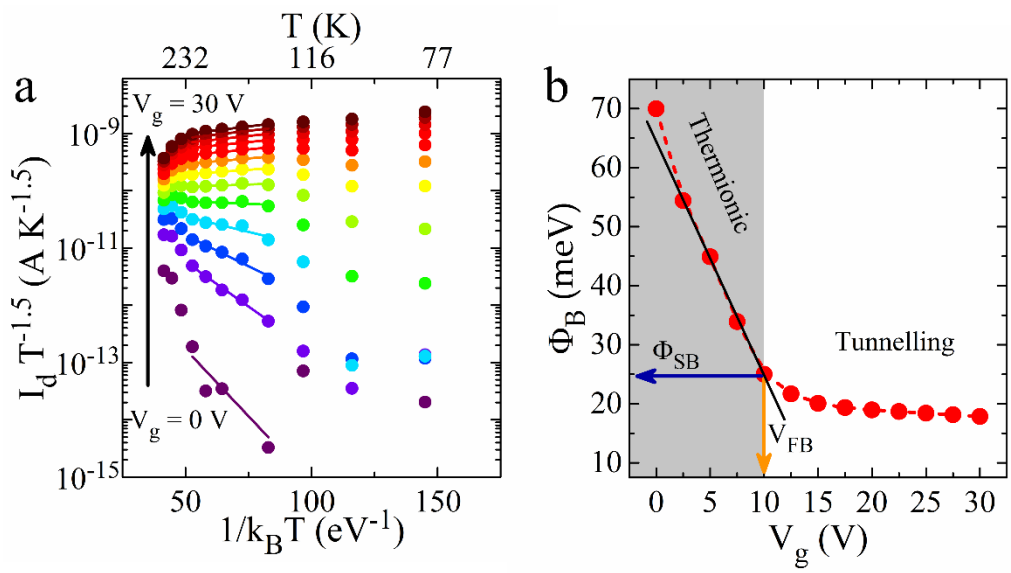

Figure S2: Thermionic emission and Schottky barrier: a) plot of $I_dT^{-1.5}$ in logarithmic scale as a function of $1/k_BT$ for various applied gate voltages ranging from 0 V to 30 V. b) Apparent barrier height (Φ_B) as function of applied gate voltage (V_g).

Apparent barrier height (Φ_B) was extracted from slope of linear fits of Figure S2a and it is shown in Figure S2b as function of applied gate voltage (V_g). Flat band voltage was estimated to be V_{FB} ~ 10 V (denoted by orange line in Figure S2b) which correspond to Schottky barrier height to be Φ_{SB} ~ 25 meV. Value of Φ_{SB} obtained for our device is smaller than Φ_{SB} of FETs based on 2D materials.[9] This might due to the fact that work function of chromium (W_{Cr} = 4.5 eV) is close to Fermi energy level of $CuIn_7Se_{11}$. Lower value of Schottky barrier height implies that charge transport in our $CuIn_7Se_{11}$ FETs is primarily governed by localized states and contact plays minimum role.

III. Density of trap states

We have used subthreshold swing (SS) to estimated density of mid-gap states (N_{tr}) which acts as localized charge trap states. SS of a FET device can be written as shown in Equation S.III.1,[10]

$$SS = \ln(10)\frac{k\,T}{e}\left(1 + \frac{C_d}{C_{ox}}\right) \tag{S.III.1}$$

where all symbols carry their usual meaning (please see main manuscript for additional details) and C_d is depletion layer capacitance. In general, depletion layer can be formed by either p-n junction or trapping of charge carrier in mid-gap states (usually referred as localized / trap states). Here we found that output characteristics (I_d - V_d) are linear, indicating that junctions (p-n and Schottky) does not play any significant role in charge transport. In presence of trap states and under assumption that density of these states does not depend on energy, SS can be written as shown in Equation S.III.2,[11, 12]

$$SS = \ln(10)\frac{k\,T}{e}\left(1 + \frac{e^2 N_{tr}}{C_{ox}}\right) \tag{S.III.2}$$

For T = 280 K, SS ~ 2.4 V/dec which correspond to $N_{tr} \sim 3 \times 10^{12}$ cm^{-2} eV^{-1}.

In order to verify trap dominated conduction at low temperatures, we estimated density of localized trap states (N_{tr}) at each temperature from subthreshold swing. At 280 K, N_{tr} was estimated to be ~ 3×10^{12} cm^{-2} eV^{-1}. We found that N_{tr} decreases as temperature decreases, reaching minimum value of ~ 1.3×10^{12} cm^{-2} eV^{-1} at 220 K, followed by abrupt increase by an order of magnitude (~ 1×10^{13}). This abrupt increase might correspond to the fact that, for T < 200 K, transport occurs through hopping between localized trap states and it is not governed by electron-phonon interaction or electrons in extended states.

IV. Critical charge density for MIT in 2D Materials

Table S1: Effective mass and critical charge density of multi-layer 2D materials exhibiting metal-insulator transition (MIT) with SiO_2 as a back gate. Here, m* - effective electron mass in units of the free electron mass (m_e), n_C - critical charge density, † - average value of n_C over a temperature range of 20 K < T < 300 K, # - *p*-type transport with graphene contact, ionic liquid on top, Φ - quantum phase transition, Λ – to our knowledge effective mass for $CuIn_7Se_{11}$ has yet to be reported so we have used effective mass of $CuInSe_2$.[13]

Materials	m* (m_e)	n_C (cm^{-2})	Ref
MoS_2 [Φ]	0.59 [14]	3.37×10^{12}	15
$MoSe_2$	0.52 [14]	$\sim 1 \times 10^{12}$	16
WSe_2 [#]	0.99 [14]	$\sim 1 \times 10^{12}$	17
$ReSe_2$ [Φ]	1.08 [18]	$\sim 3 \times 10^{12}$	19
$CuIn_7Se_{11}$ [Λ]	0.09 [13]	[†] 2.66×10^{11}	This Work
$CuIn_7Se_{11}$ [Λ]	0.09 [13]	[†] 3.28×10^{11}	This Work

V. Percolation analysis of device II

In case of device II, as shown in Figure S3, α ~ 1.6 at temperatures close to 300 K, which indicates partial screening of the Coulomb impurities[20] and as temperature decreases, α steadily increases reaching α ~ 2 at temperatures T < 100 K which indicates bare Coulomb impurity scattering.[20] For device II at 300 K, δ ~ 1.29 and $n_C \sim 1.7 \times 10^{12}$ cm^{-1}.

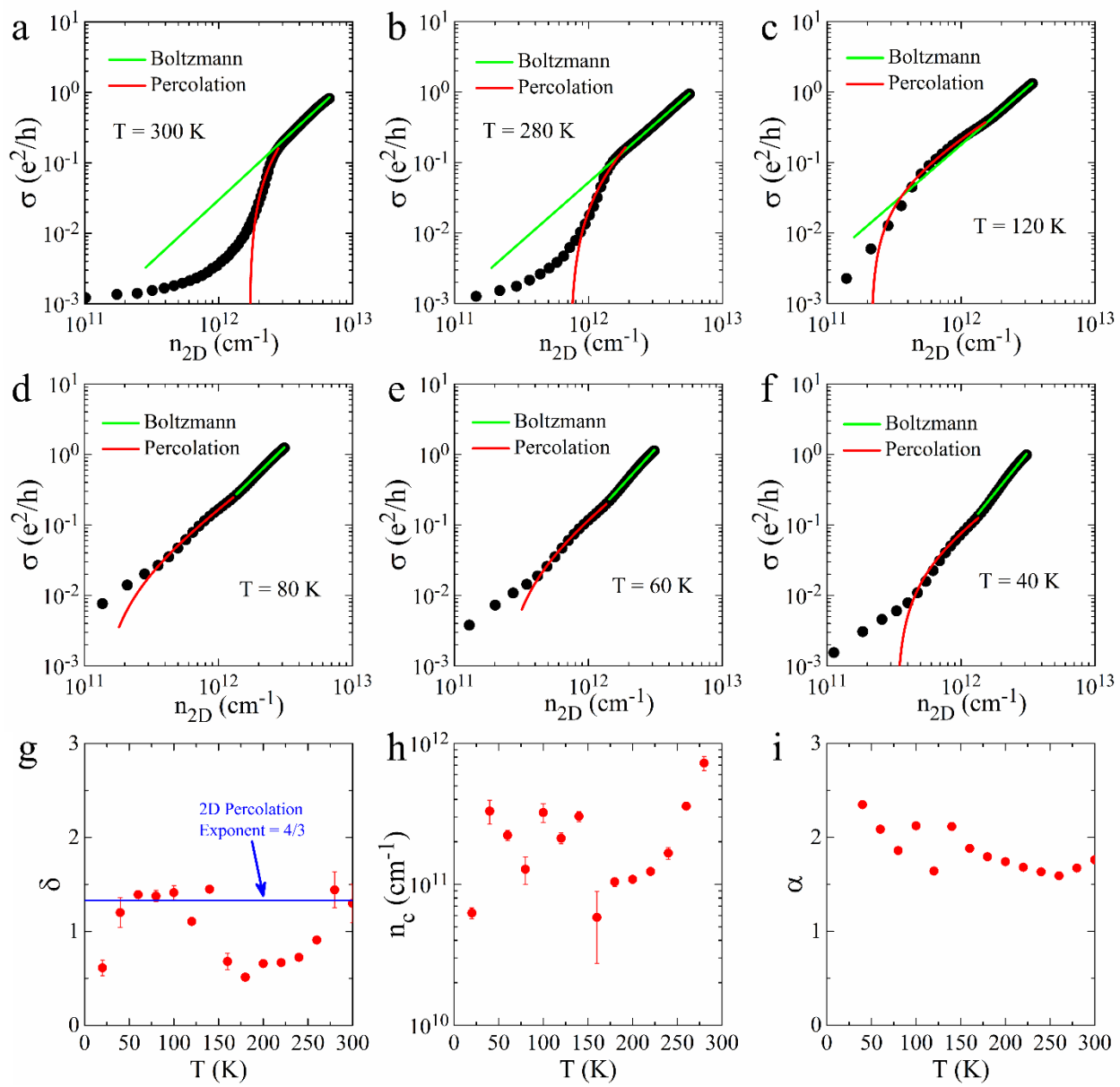

Figure S3: Conductivity (σ) as a function of charge carrier density (n_{2D}) for device II at T = a) 300 K, b) 280 K, c) 120 K, d) 80 K, e) 60 K and f) 40 K. Green curve represents Boltzmann theory fit of form $\sigma(n) \propto n^{\alpha}$ and red curve represents percolation critical behavior of form $\sigma(n) = A(n - n_C)^{\delta}$. g) Critical percolation exponent δ(T), h) critical density n_C (T) and i) conductivity exponent α(T) for device II.

REFERENCES

1. Ghibaudo, G., New Method for the Extraction of MOSFET Parameters. *Electron. Lett.* **1988,** *24* (9), 543-545.
2. Chang, H.-Y.; Zhu, W.; Akinwande, D., On the Mobility and Contact Resistance Evaluation for Transistors Based on MoS_2 or Two-Dimensional Semiconducting Atomic Crystals. *Appl. Phys. Lett.* **2014,** *104* (11), 113504.
3. Pérez-Tomás, A.; Placidi, M.; Fontserè, A.; Gammon, P. M.; Jennings, M. R., Temperature Behavior and Modeling of Ohmic Contacts to Si+ Implanted *n*-Type GaN. *Microelectron. Reliab.* **2011,** *51* (8), 1325-1329.
4. Houssa, M.; Dimoulas, A.; Molle, A., 2D Materials for Nanoelectronics. *CRC Press*, Boca Raton, **2016**.
5. Wei, X.; Chen, Q.; Peng, L., Electron Emission from a Two-Dimensional Crystal with Atomic Thickness. *AIP Adv.* **2013,** *3* (4), 042130.
6. Li, X.; Grassi, R.; Li, S.; Li, T.; Xiong, X.; Low, T.; Wu, Y., Anomalous Temperature Dependence in Metal–Black Phosphorus Contact. *Nano Lett.* **2018,** *18* (1), 26-31.
7. Cheung, S. K.; Cheung, N. W., Extraction of Schottky Diode Parameters from Forward Current-Voltage Characteristics. *Appl. Phys. Lett.* **1986,** *49* (2), 85-87.
8. Al-Asadi, A. S.; Henley, L. A.; Ghosh, S.; Quetz, A.; Dubenko, I.; Pradhan, N.; Balicas, L.; Perea-Lopez, N.; Carozo, V.; Lin, Z.; Terrones, M.; Talapatra, S.; Ali, N., Fabrication and Characterization of Ultraviolet Photosensors from ZnO Nanowires Prepared Using Chemical Bath Deposition Method. *J. Appl. Phys.* **2016,** *119* (8), 084306.
9. Das, S.; Chen, H.-Y.; Penumatcha, A. V.; Appenzeller, J., High Performance Multilayer MoS_2 Transistors with Scandium Contacts. *Nano Lett.* **2013,** *13* (1), 100-105.
10. Sze, S. M.; Ng, K. K., Physics of Semiconductor Devices. *John wiley & sons*, Hoboken, **2006**.
11. Kim, H.; Kim, D.; Jeong, C.; Lee, J.; Kwon, H., Determination of Interface and Bulk Trap Densities in High-Mobility *p*-Type WSe_2 Thin-Film Transistors. *IEEE Electron Device Lett.* **2017,** *38* (4), 481-484.
12. Kalb, W. L.; Batlogg, B., Calculating the Trap Density of States in Organic Field-Effect Transistors from Experiment: a Comparison of Different Methods. *Phys. Rev. B* **2010,** *81* (3), 035327.
13. Gadzhiev, T. M.; Babaev, A. A.; Gadzhieva, R. M.; Magomedova, D. K.; Khokhlachev, P. P., Properties of $CuInSe_2$ Films Obtained by Methods of Selenization and Quasi-Equilibrium Deposition. *Inorg. Mater.* **2008,** *44* (12), 1295.
14. Wickramaratne, D.; Zahid, F.; Lake, R. K., Electronic and Thermoelectric Properties of Few-Layer Transition Metal Dichalcogenides. *J. Chem. Phys.* **2014,** *140* (12), 124710.
15. Moon, B. H.; Bae, J. J.; Joo, M.-K.; Choi, H.; Han, G. H.; Lim, H.; Lee, Y. H., Soft Coulomb Gap and Asymmetric Scaling Towards Metal-Insulator Quantum Criticality in Multilayer MoS_2. *Nat. Commun.* **2018,** *9* (1), 2052.
16. Chamlagain, B.; Li, Q.; Ghimire, N. J.; Chuang, H.-J.; Perera, M. M.; Tu, H.; Xu, Y.; Pan, M.; Xaio, D.; Yan, J.; Mandrus, D.; Zhou, Z., Mobility Improvement and Temperature Dependence in $MoSe_2$ Field-Effect Transistors on Parylene-C Substrate. *ACS Nano* **2014,** *8* (5), 5079-5088.
17. Chuang, H.-J.; Tan, X.; Ghimire, N. J.; Perera, M. M.; Chamlagain, B.; Cheng, M. M.-C.; Yan, J.; Mandrus, D.; Tománek, D.; Zhou, Z., High Mobility WSe_2 *p*- and *n*-Type Field-

Effect Transistors Contacted by Highly Doped Graphene for Low-Resistance Contacts. *Nano Lett.* **2014,** *14* (6), 3594-3601.
18. Kim, B. S.; Kyung, W. S.; Denlinger, J. D.; Kim, C.; Park, S. R., Strong One-Dimensional Characteristics of Hole-Carriers in ReS_2 and $ReSe_2$. *Sci. Rep.* **2019,** *9* (1), 2730.
19. Pradhan, N. R.; McCreary, A.; Rhodes, D.; Lu, Z.; Feng, S.; Manousakis, E.; Smirnov, D.; Namburu, R.; Dubey, M.; Hight Walker, A. R.; Terrones, H.; Terrones, M.; Dobrosavljevic, V.; Balicas, L., Metal to Insulator Quantum-Phase Transition in Few-Layered ReS_2. *Nano Lett.* **2015,** *15* (12), 8377-8384.
20. Ghatak, S.; Pal, A. N.; Ghosh, A., Nature of Electronic States in Atomically Thin MoS_2 Field-Effect Transistors. *ACS Nano* **2011,** *5* (10), 7707-7712.